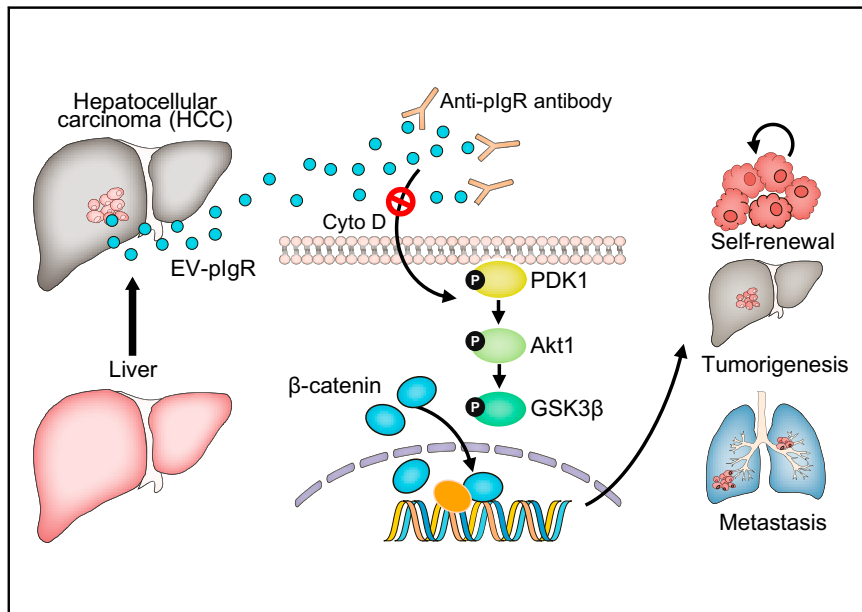


# Patient pIgR-enriched extracellular vesicles drive cancer stemness, tumorigenesis and metastasis in hepatocellular carcinoma

## Graphical abstract



## Authors

Sze Keong Tey, Samuel Wan Ki Wong, Janice Yuen Tung Chan, ..., Yi Gao, Jing Ping Yun, Judy Wai Ping Yam

## Correspondence

[judyam@pathology.hku.hk](mailto:judyam@pathology.hku.hk)  
(J.W.P. Yam).

## Lay summary

The World Health Organization estimates that more than 1 million patients will die from liver cancer, mostly hepatocellular carcinoma (HCC), in 2030. Understanding the underlying mechanism by which HCC acquires aggressive attributes is crucial to improving the diagnosis and treatment of patients. Herein, we demonstrated that nanometer-sized extracellular vesicles released by tumors promote cancer stemness and tumorigenesis. Within these oncogenic vesicles, we identified a key component that functions as a potent modulator of cancer aggressiveness. By inhibiting this functional component of EVs using a neutralizing antibody, tumor growth was profoundly attenuated in mice. This hints at a potentially effective therapeutic alternative for patients with cancer.

## Highlights

- Elevated pIgR levels are found in circulating extracellular vesicles from patients with liver cancer.
- EV-pIgR promotes cancer stemness and cancerous phenotypes in recipient liver cancer cells.
- EV-pIgR promotes liver cancer cell aggressiveness by activating the PDK1/Akt/GSK3β/β-catenin signaling axis.
- Combined treatment using sorafenib and anti-pIgR antibody attenuates growth of patient-derived xenografts in mice.



# Patient pIgR-enriched extracellular vesicles drive cancer stemness, tumorigenesis and metastasis in hepatocellular carcinoma

Sze Keong Tey<sup>1,†</sup>, Samuel Wan Ki Wong<sup>1,†</sup>, Janice Yuen Tung Chan<sup>1</sup>, Xiaowen Mao<sup>1</sup>, Tung Him Ng<sup>1</sup>, Cherlie Lot Sum Yeung<sup>1</sup>, Zoe Leung<sup>1</sup>, Hiu Ling Fung<sup>1</sup>, Alexander Hin Ning Tang<sup>1</sup>, Danny Ka Ho Wong<sup>2,3</sup>, Lung-Yi Mak<sup>2,3</sup>, Man-Fung Yuen<sup>2,3</sup>, Chun-Fung Sin<sup>1</sup>, Irene Oi-Lin Ng<sup>1,3</sup>, Stephanie Kwai Yee Ma<sup>3,4</sup>, Terence Kin Wah Lee<sup>5</sup>, Peihua Cao<sup>6,7</sup>, Kebo Zhong<sup>7</sup>, Yi Gao<sup>7</sup>, Jing Ping Yun<sup>8</sup>, Judy Wai Ping Yam<sup>1,3,\*</sup>

<sup>1</sup>Department of Pathology, Li Ka Shing Faculty of Medicine, The University of Hong Kong, Hong Kong; <sup>2</sup>Department of Medicine, Li Ka Shing Faculty of Medicine, The University of Hong Kong, Hong Kong; <sup>3</sup>State Key Laboratory of Liver Research (The University of Hong Kong), Hong Kong; <sup>4</sup>School of Biomedical Sciences, Li Ka Shing Faculty of Medicine, The University of Hong Kong, Hong Kong; <sup>5</sup>Department of Applied Biology and Chemical Technology, The Hong Kong Polytechnic University, Hong Kong; <sup>6</sup>Clinical Research Center, Zhujiang Hospital, Southern Medical University, Guangzhou, Guangdong, PR China; <sup>7</sup>Department of Hepatobiliary Surgery II, Zhujiang Hospital, Southern Medical University, Guangzhou, Guangdong, PR China; <sup>8</sup>Department of Pathology, Sun Yat-sen University Cancer Center, Guangzhou, Guangdong, PR China

See Editorial, pages 768–770

**Background & Aims:** Extracellular vesicles (EVs) play a pivotal role in connecting tumor cells with their local and distant microenvironments. Herein, we aimed to understand the role (on a molecular basis) patient-derived EVs play in modulating cancer stemness and tumorigenesis in the context of hepatocellular carcinoma (HCC).

**Methods:** EVs from patient sera were isolated, quantified and characterized. The EVs were vigorously tested, both *in vitro* and *in vivo*, through various functional assays. Proteomic analysis was performed to identify the functional components of EVs. The presence and level of polymeric immunoglobulin receptor (pIgR) in circulating EVs and tumor and non-tumorous tissues of patients with HCC were determined by ELISA, immunoblotting, immunohistochemistry and quantitative PCR. The functional role and underlying mechanism of EVs with enhanced pIgR expression were elucidated. Blockade of EV-pIgR with neutralizing antibody was performed in nude mice implanted with patient-derived tumor xenografts (PDXs).

**Results:** Circulating EVs from patients with late-stage HCC (L-HCC) had significantly elevated pIgR expression compared to the EVs released by control individuals. The augmenting effect of L-HCC-EVs on cancer stemness and tumorigenesis was hindered by an anti-pIgR antibody. EVs enriched with pIgR consistently promoted cancer stemness and cancerous phenotypes in recipient cells. Mechanistically, EV-pIgR-induced cancer aggressiveness was abrogated by Akt and  $\beta$ -catenin inhibitors, confirming that the role of EV-pIgR depends on the activation of the PDK1/Akt/GSK3 $\beta$ / $\beta$ -

catenin signaling axis. Furthermore, an anti-pIgR neutralizing antibody attenuated tumor growth in mice implanted with PDXs.

**Conclusions:** This study illustrates a previously unknown role of EV-pIgR in regulating cancer stemness and aggressiveness: EV-pIgR activates PDK1/Akt/GSK3 $\beta$ / $\beta$ -catenin signaling cascades. The blockade of the intercellular communication mediated by EV-pIgR in the tumor microenvironment may provide a new therapeutic strategy for patients with cancer.

**Key summary:** The World Health Organization estimates that more than 1 million patients will die from liver cancer, mostly hepatocellular carcinoma (HCC), in 2030. Understanding the underlying mechanism by which HCC acquires aggressive attributes is crucial to improving the diagnosis and treatment of patients. Herein, we demonstrated that nanometer-sized extracellular vesicles released by tumors promote cancer stemness and tumorigenesis. Within these oncogenic vesicles, we identified a key component that functions as a potent modulator of cancer aggressiveness. By inhibiting this functional component of EVs using a neutralizing antibody, tumor growth was profoundly attenuated in mice. This hints at a potentially effective therapeutic alternative for patients with cancer.

© 2021 The Author(s). Published by Elsevier B.V. on behalf of European Association for the Study of the Liver. This is an open access article under the CC BY-NC-ND license (<http://creativecommons.org/licenses/by-nc-nd/4.0/>).

## Introduction

Hepatocellular carcinoma (HCC) accounts for the majority of primary liver cancers and is currently the fourth leading cause of cancer-related death worldwide.<sup>1</sup> HCC is often diagnosed at an advanced stage, thus precluding curative surgical resection. Therapeutic options for advanced HCC are limited in availability and efficacy. Therefore, understanding how HCC acquires aggressive traits is important to revamp the current state of early diagnosis and treatment.

Keywords: Liver cancer; Tumor microenvironment; Intercellular communication; Proteomics; Neutralizing antibody.

Received 24 April 2021; received in revised form 24 November 2021; accepted 7 December 2021; available online 16 December 2021

\* Corresponding author. Address: Department of Pathology, 7/F Block T, Queen Mary Hospital, Pokfulam, Hong Kong, China; Tel.: 852-22552681, fax: 852-22185212.

E-mail address: [judyam@pathology.hku.hk](mailto:judyam@pathology.hku.hk) (J.W.P. Yam).

<sup>†</sup> Contributed equally

<https://doi.org/10.1016/j.jhep.2021.12.005>



ELSEVIER

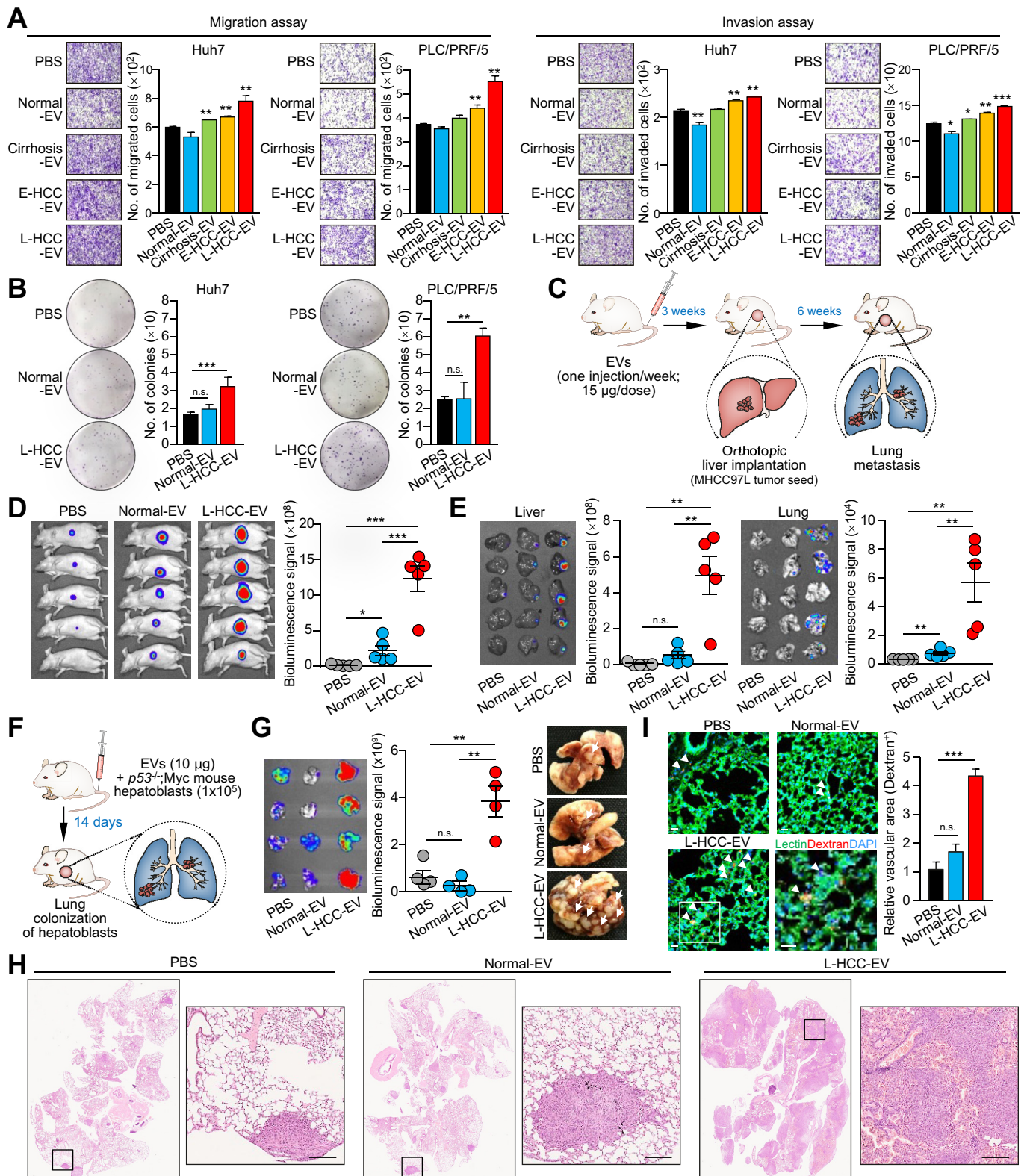


**Fig. 1. Circulating EVs from patients with HCC promote HCC cell aggressiveness.** (A) Migration and invasion assays of HCC cells pretreated with the indicated EVs. (B) Colony formation assay of EV-treated cells. (C) Schematic diagram of the EV education model. (D) Bioluminescence imaging of animals at the end of the experiment (n = 5). (E) Ex vivo bioluminescence imaging of liver and lung tissues. (F) Schematic diagram of the experimental metastasis assay. (G) Bioluminescence imaging of excised lungs (left). The intensity of signals in the lung were plotted (middle). Image of lungs after fixation (right). Tumor nodules are indicated by arrows. (H) H&E staining of lung tissues. Scale bar, 200  $\mu$ m. (I) Analysis of lung vessel leakiness. Arrowhead indicates areas with diffused dextran. Scale bar: 20  $\mu$ m. Data are presented as the mean  $\pm$  SEM. Student's *t* test was used for 2 groups. \**p* < 0.05; \*\**p* < 0.01; \*\*\**p* < 0.001; n.s., not significant. Cirrhosis-EV, EV from patients with HBV-related cirrhosis; E-HCC-EV, EV from patients with early HCC; EVs, extracellular vesicles; HCC, hepatocellular carcinoma; L-HCC-EVs, EVs from patients with late HCC; Normal-EV, EVs from healthy individuals.

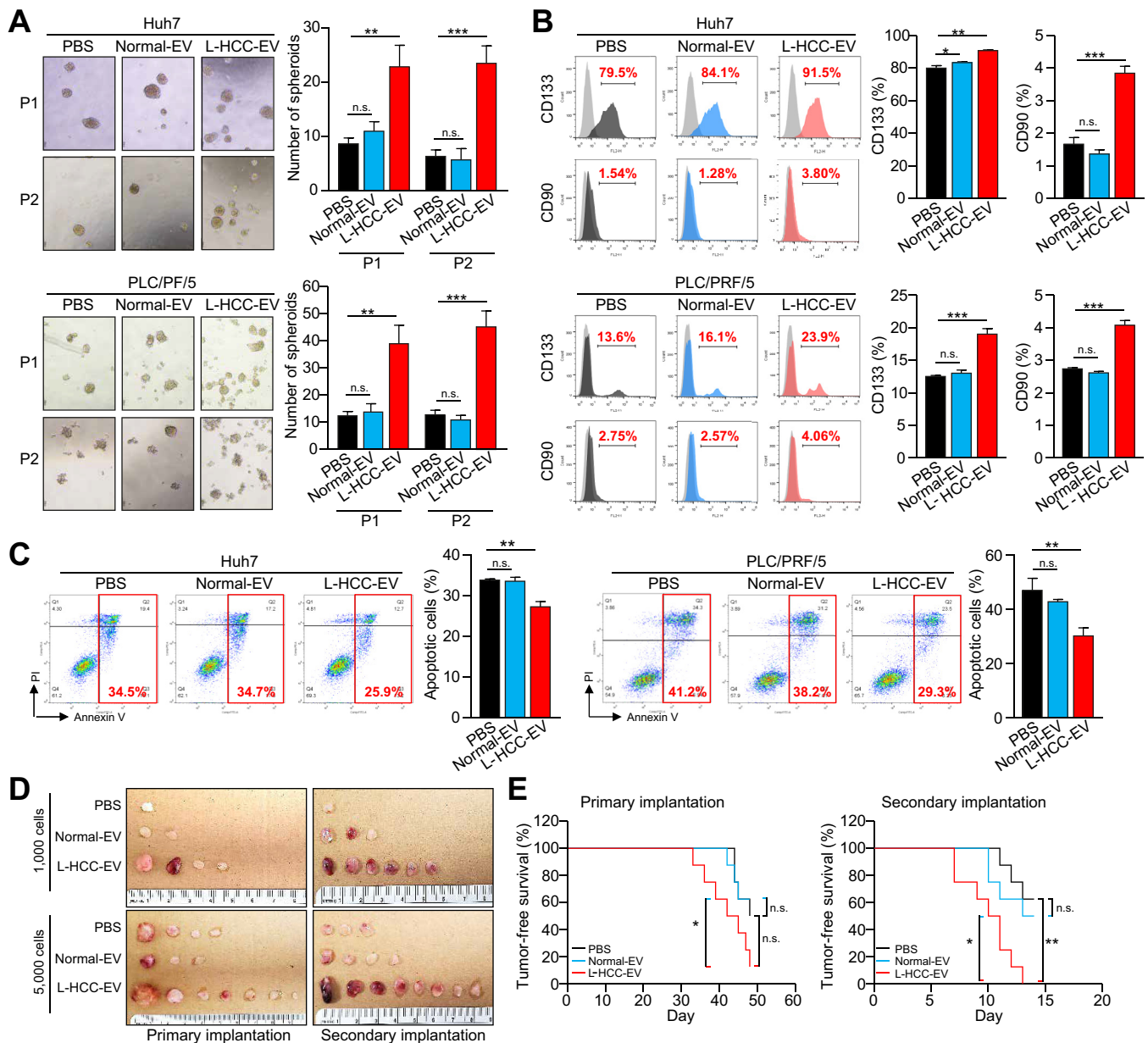


**Fig. 2. Circulating EVs from patients with late-stage HCC enhance the cancer stemness properties of HCC cells.** (A) Hepatosphere formation and serial passage of HCC cells pretreated with the indicated EVs before plating. Representative photographs of spheroids formed after incubation. The histogram indicates the number of spheres formed per 1,000 cells. P1 and P2 represent passage 1 and 2, respectively. (B) Flow cytometry analysis of CD90 and CD133 expression in HCC cells treated with PBS or EVs. (C) Apoptosis assay in which EVs and sorafenib-treated cells were stained with PI and annexin V-FITC. Flow cytometry was conducted to determine the percentage of apoptotic cells. (D) Image of tumors formed by 1,000 and 5,000 PLC/PRF/5 cells treated with or without EVs before subcutaneous injection into NOD/SCID mice ( $n = 8$ ). (E) Tumor-free survival curves of mice injected with 5,000 cells in the primary (left) and secondary (right) implantation are shown. Data are presented as the mean  $\pm$  SEM. Student's  $t$  test was used for 2 groups, and a log-rank (Mantel-Cox) test was used for survival curves. \* $p < 0.05$ ; \*\* $p < 0.01$ ; \*\*\* $p < 0.001$ ; n.s., not significant. EVs, extracellular vesicles; HCC, hepatocellular carcinoma; L-HCC-EVs, EVs from patients with late HCC; Normal-EV, EVs from healthy individuals; PI, propidium iodide.

Growing evidence has revealed that intercellular communication is mediated not only by direct cellular contact and soluble factors, but also by extracellular vesicles (EVs). EVs are membrane-derived nanometer-sized vesicles that function by transferring donor cell-derived bioactive molecules, including lipids, nucleic acids and proteins, into recipient cells. The tumor microenvironment is a heterogeneous and composite milieu that supports cancer cell growth, survival and metastasis. Evidently,

cancer cell-derived EVs are critical messengers that connect tumor cells with their local and distant microenvironments, orchestrating multiple systemic pathophysiological processes to facilitate cancer progression.

Despite the multifarious effect of EVs in cancer development, the role of EVs associated with cancer stem cells (CSCs) remains uncertain, and the function of EVs in hepatic CSCs is scarcely reported. In a chemically induced HCC rat model, EVs derived

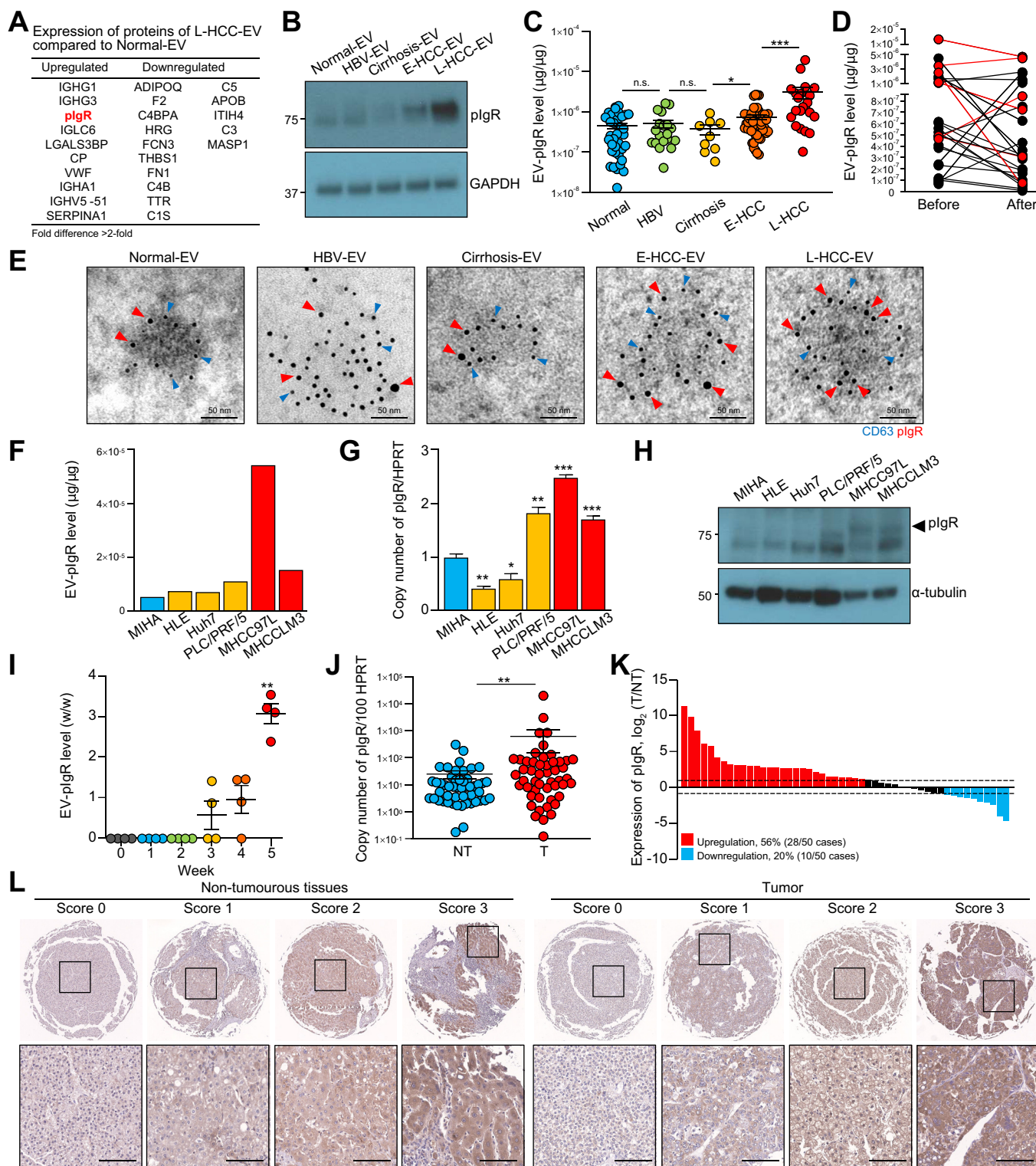


**Fig. 3. plgR-enriched circulating EVs are found in patients with HCC.** (A) Proteins modulated by >2-fold in L-HCC-EVs when compared to Normal-EVs analyzed from proteomic profiling are listed. (B) Immunoblot showing plgR expression in the indicated EVs, with GAPDH as the loading standard. (C) ELISA of plgR levels in circulating EVs from control individuals (Normal, n = 36) and patients with HBV (HBV, n = 20), HBV-related cirrhosis (Cirrhosis, n = 9), early HCC (E-HCC, n = 49) or late HCC (L-HCC, n = 22). (D) Determination of EV-plgR in patients with HCC before and after surgery (n = 25). Late-stage cases are indicated in red and early-stage cases are marked in black. (E) Representative electron micrograph of EVs subjected to immunogold labeling using anti-CD63 and anti-plgR antibodies followed by secondary antibodies conjugated to 5 and 10 nm gold particles, respectively. Scale bar: 50 nm. (F) The expression of plgR in EVs obtained from conditioned medium of cells was analyzed via ELISA. The expression of plgR in normal liver cell line (blue) and non-metastatic (orange) and metastatic (red) HCC cell lines was determined using qPCR (G) and western blotting (H). (I) plgR levels in circulating EVs collected from mice implanted with MHCC97L tumor seeds in the liver (n = 4). (J) plgR mRNA expression in 50 paired T and NT liver tissues was determined by qPCR. (K) Relative fold change in plgR mRNA expression between T and NT liver tissues (n = 50). A fold difference >2 was considered to indicate upregulation or downregulation. (L) Representative

from hepatic CSCs augmented tumor growth and metastasis.<sup>2</sup> In addition, EVs derived from CD90<sup>+</sup> liver cancer cells modulated endothelial cells to facilitate angiogenesis in HCC.<sup>3</sup> The significant impact of CSCs and EVs in HCC underscores the need for a better understanding of the link between EVs and liver CSCs.

Polymeric immunoglobulin receptor (pIgR) is widely expressed in mucosal epithelial cells and regulates transcytosis of dimeric IgA and pentameric IgM, which are the first-line antibodies against initial infection. Expression of pIgR is upregulated by proinflammatory cytokines upon viral or bacterial infection, thus bridging innate and adaptive immunity.<sup>4</sup> Emerging findings have revealed the aberrant expression of pIgR in cancerous tissues. However, the clinical relevance and functions of pIgR in tumor cells remain uncertain. Intriguingly, studies have yet to report on the functional role of pIgR when expressed by tumor-derived EVs. For the first time, we identified pIgR as a key molecule that confers oncogenic effects on circulating EVs from patients with HCC. Herein, we uncover the role of pIgR-enriched EVs in enhancing cancer stemness and aggressiveness, and provide insight into the clinical relevance of pIgR as a promising biomarker and therapeutic target in HCC.

## Materials and methods

### Human samples

Serum samples were randomly collected from healthy donors with non-liver disease backgrounds (as controls), individuals with chronic HBV infection and individuals with liver disease (cirrhosis, early HCC and late HCC) who had not received any treatment. Information on serum donors is listed in Table S1. The collection of serum samples was executed at Queen Mary Hospital, Hong Kong and Zhujiang Hospital, Guangzhou, China with informed consent from all donors. Procedure approval was obtained from the Institutional Review Board of The University of Hong Kong/Hospital Authority Hong Kong West Cluster (HKU/HA HKW IRB) and Zhujiang Hospital of Southern Medical University. All experiments involving human samples were handled in accordance with relevant ethical regulations.

### Statistical analysis

The readings of all assays were calculated as the mean ± SEM. Student's *t* test, ANOVA and log-rank (Mantel-Cox) tests performed using Prism software (version 8.0.1, GraphPad) were used for statistical analysis. A *p* value of less than 0.05 was considered statistically significant.

For further details regarding the materials and methods used, please refer to the CTAT table and supplementary information.

## Results

### HCC patient-derived EVs promote aggressive phenotypes in HCC cells

EVs derived from HCC cell lines have been shown to play pivotal roles in enhancing HCC aggressiveness<sup>5,6</sup>; however, the physiological relevance of their functional effect in patients remains ambiguous. Circulating EVs were collected from healthy

individuals (Normal-EVs), and from patients with chronic HBV infection, HBV-related cirrhosis, early HCC (E-HCC-EVs) or late HCC (L-HCC-EVs) for functional analyses. Based on the Minimal Information for Studies of Extracellular Vesicles (MISEV) guidelines,<sup>7</sup> the isolated EVs were validated by their expression of small EV markers, size and morphology (Fig. S1A-S1C). Notably, the greatest amount of EVs was obtained from late-stage patients compared to other serum donors (Fig. S1D).

EVs from patients with HCC but not Normal-EVs increased the growth and motility of Huh7 and PLC/PRF/5 cells (Fig. S2A-S2D). Compared to Normal-, Cirrhosis- and E-HCC-EVs, L-HCC-EVs exhibited the highest potency in promoting cell migration, invasiveness and colony formation (Fig. 1A-B) and in enhancing tumor development (Fig. S2E). In an orthotopic liver implantation model, repeated injection of L-HCC-EVs into mice resulted in enhanced liver tumor formation and distant lung metastasis (Fig. 1C-E). A consistent effect of L-HCC-EVs in promoting metastasis was observed in an experimental metastasis assay involving coinjection of EVs and murine p53<sup>-/-</sup>;Myc-transduced hepatoblasts (Fig. 1F-H). L-HCC-EVs were shown to reduce expression of the tight junction protein VE-cadherin in human umbilical vein endothelial cells (Fig. S3) and enhance endothelial permeability in mice (Fig. 1I). These findings suggest that the promotion of metastasis could be ascribed to leakiness in the pulmonary vasculature induced by L-HCC-EVs, thus facilitating extravasation and colonization of tumor cells in the lungs.

### HCC patient-derived EVs promote cancer stemness in HCC cells

In addition to modulating the cancer phenotypes of tumor cells, L-HCC-EVs increased the cancer stemness properties of HCC cells. HCC cells treated with L-HCC-EVs but not Normal-EVs showed a marked increase in the ability to form tumorspheres in a spheroid formation assay (Fig. 2A) and enhanced expression of the CSC markers CD90 and CD133 (Fig. 2B). L-HCC-EVs also increased the expression of CD24, CD47 and EpCAM in Huh7 cells but not in PLC/PRF/5 cells (Fig. S4). In addition, L-HCC-EVs reduced the sensitivity of cells to sorafenib (Fig. 2C). Limiting dilution analysis performed in NOD/SCID mice showed that HCC cells treated with L-HCC-EVs displayed a significant enhancement in tumorigenicity, with an increased tumor incidence, shorter tumor latency and increased estimated tumor-initiating cell frequency compared to cells treated with PBS or Normal-EVs (Table S2). The self-renewal ability of L-HCC-EV-treated cells was further expedited as revealed by serial transplantation of primary xenografts into secondary mouse recipients (Fig. 2D). L-HCC-EV-treated cells showed significantly worse tumor-free survival than cells treated with PBS or Normal-EVs after both primary and secondary implantation (Fig. 2E).

### pIgR is upregulated in circulating EVs of patients with HCC

To ascertain differences in biological activities between EVs of healthy controls and those of patients, their proteomic profiles were compared. Among candidates that were modulated by at

images of pIgR expression with intensity scores (0-3). Scale bar, 100 μm. (M) The number of cases with each intensity score (left) and the H-scores of pIgR expression (right) were plotted (n = 143). (N) Representative cases with pIgR overexpression. Scale bar, 100 μm. Alteration of pIgR expression in paired samples are depicted in the pie chart. Data are presented as the mean ± SEM. Student's *t* test for 2 groups was used. \**p* < 0.05; \*\**p* < 0.01; \*\*\**p* < 0.001; n.s., not significant. Cirrhosis-EV, EV from patients with HBV-related cirrhosis; E-HCC-EV, EV from patients with early HCC; EVs, extracellular vesicles; HCC, hepatocellular carcinoma; L-HCC-EVs, EVs from patients with late HCC; Normal-EV, EVs from healthy individuals; NT, non-tumorous; pIgR, polymeric immunoglobulin receptor; T, tumor.

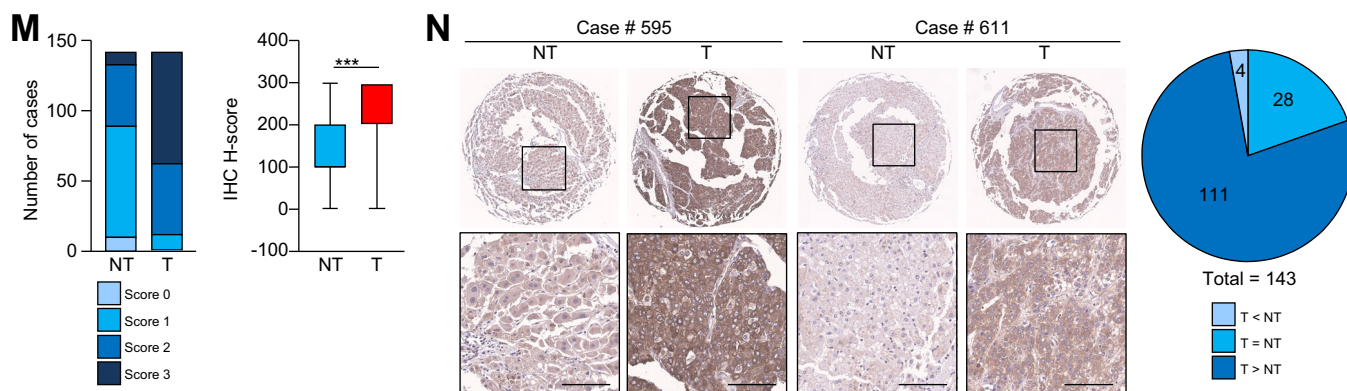


Fig. 3.

least 2-fold in L-HCC-EVs compared to Normal-EVs, pIgR – which has been implicated in HCC<sup>8,9</sup> – was chosen for further investigation (Fig. 3A). Upregulation of pIgR in E-HCC- and L-HCC-EVs was corroborated by immunoblotting (Fig. 3B). A significant increase in pIgR was consistently detected in a cohort of patients' circulating EVs (Fig. 3C). The level of EV-pIgR was reduced in 72% (18/25) of patients after surgery (Fig. 3D). Immunogold labeling revealed the presence of pIgR on the surface of CD63+ circulating EVs (Fig. 3E). A higher level of pIgR was detected in EVs from metastatic HCC cells than in EVs from normal liver and non-metastatic cells (Fig. 3F). Similar pIgR expression profiles were also observed at both the transcript (Fig. 3G) and protein (Fig. 3H) level in HCC cell lines. In mice implanted with tumor seeds derived from metastatic MHCC97L cells, the level of circulating EV-pIgR progressively increased during tumor development (Fig. 3I). These data indicate that tumors were likely the major source of EV-pIgR and that its level could be an indicator of tumor development. Similar to EV-pIgR, overall *pIgR* mRNA expression was significantly upregulated in tumorous tissues compared to non-tumorous tissues (Fig. 3J). Notably, the *pIgR* transcript was upregulated in 56% (28/50) of patients with HCC (Fig. 3K). In a tissue microarray comprising 143 paired HCC samples, strong (score 3) and moderate (score 2) positive staining of pIgR was detected in 91.6% (131/143) of tumorous tissues, whereas 62.9% (90/143) of non-tumorous tissues showed weak positive (score 1) or negative staining (score 0) (Fig. 3L-M). The H-score revealed a significantly higher immunoreactivity of pIgR in tumorous tissue (Fig. 3M). Frequent overexpression of pIgR was found in 77.6% (111/143) of cases (Fig. 3N).

#### pIgR is functionally responsible for the tumor-promoting effect of HCC patient-derived EVs

Due to the presence of pIgR on the surface of EVs (Fig. 3E), we examined whether neutralizing antibody against pIgR was able to block the tumor-promoting effect of L-HCC-EVs. Indeed, cotreatment with anti-pIgR antibody blocked the effect of L-HCC-EVs on colony formation, migration and invasion of PLC/PRF/5 cells (Fig. 4A,B). Furthermore, the metastasis of murine p53<sup>-/-</sup>;Myc-transduced hepatoblasts induced by L-HCC-EVs was significantly hindered by coinjection with anti-pIgR antibody in the experimental metastasis assay (Fig. 4C-F). Anti-pIgR antibody also abrogated L-HCC-EVs' ability to promote the *in vitro* self-renewal and the percentage of CD90- and CD133-expressing

PLC/PRF/5 cells (Fig. 4G,H), as well as to reduce the sensitivity of HCC cells to sorafenib (Fig. 4I). The augmenting activity of L-HCC-EVs was also observed in Huh7 cells and was neutralized by anti-pIgR antibody (Fig. S5). These findings suggest that circulating EVs from patients with HCC augment the cancer stemness properties of cells through the functions of pIgR.

To identify the functional role of pIgR in EVs, pIgR was stably expressed in Huh7 cells using CRISPR synergistic activation mediators (SAM-pIgR) and an EV-targeting expression vector (XP-pIgR) (Fig. S6A-S6B). EVs collected from the conditioned medium of SAM-pIgR and XP-pIgR cells showed upregulated pIgR compared to EVs collected from the respective control SAM-CTL and XP-CTL cells. The purity and integrity of the isolated EVs were validated (Fig. S6A, S6C,D). As revealed by various *in vitro* functional assays, SAM-pIgR-EVs and XP-pIgR-EVs enhanced the cancer properties of PLC/PRF/5 and Huh7 cells (Fig. 5A-C; Fig. S7A-S7C). This augmenting effect of SAM-pIgR-EVs and XP-pIgR-EVs in promoting Huh7 cell migration and invasion was abolished by the addition of anti-pIgR antibody (Fig. S7D-S7E). XP-pIgR-EVs were capable of promoting the metastasis of murine p53<sup>-/-</sup>; Myc-transduced hepatoblasts (Fig. 5D-F). Furthermore, XP-pIgR-EVs promoted *in vitro* self-renewal, increased the CD90- and CD133-expressing PLC/PRF/5 population (Fig. 5G-H) and suppressed the sensitivity of HCC cells to sorafenib (Fig. 5I). Serial transplantation assays showed that PLC/PRF/5 cells treated with XP-pIgR-EVs displayed a significant enhancement in tumorigenicity, with an increased tumor incidence, shorter tumor latency and increased estimated tumor-initiating cell frequency, compared to cells treated with PBS or XP-CTL-EVs (Table S3). The self-renewal ability of XP-pIgR-EV-treated cells was further increased in secondary implants compared to primary xenografts (Fig. 5J). XP-pIgR-EV-treated cells showed worse tumor-free survival than cells treated with PBS or XP-CTL-EVs (Fig. 5K). Taken together, these findings demonstrate that the functional capacity of EV-pIgR was consistent with the clinical results showing an upregulation of EV-pIgR in patients with HCC. Importantly, these data suggest a previously undiscovered role of EV-enriched pIgR in promoting HCC aggressiveness, which prompted us to investigate the underlying molecular basis of this observation.

#### EV-pIgR activates $\beta$ -catenin signaling through PDK1/Akt/GSK3 $\beta$ signaling

The expression of genes that are involved in cancer stemness and drug resistance regulation was analyzed in PLC/PRF/5 and Huh7 cells treated with Normal-EVs and L-HCC-EVs (Fig. 6A). L-HCC-

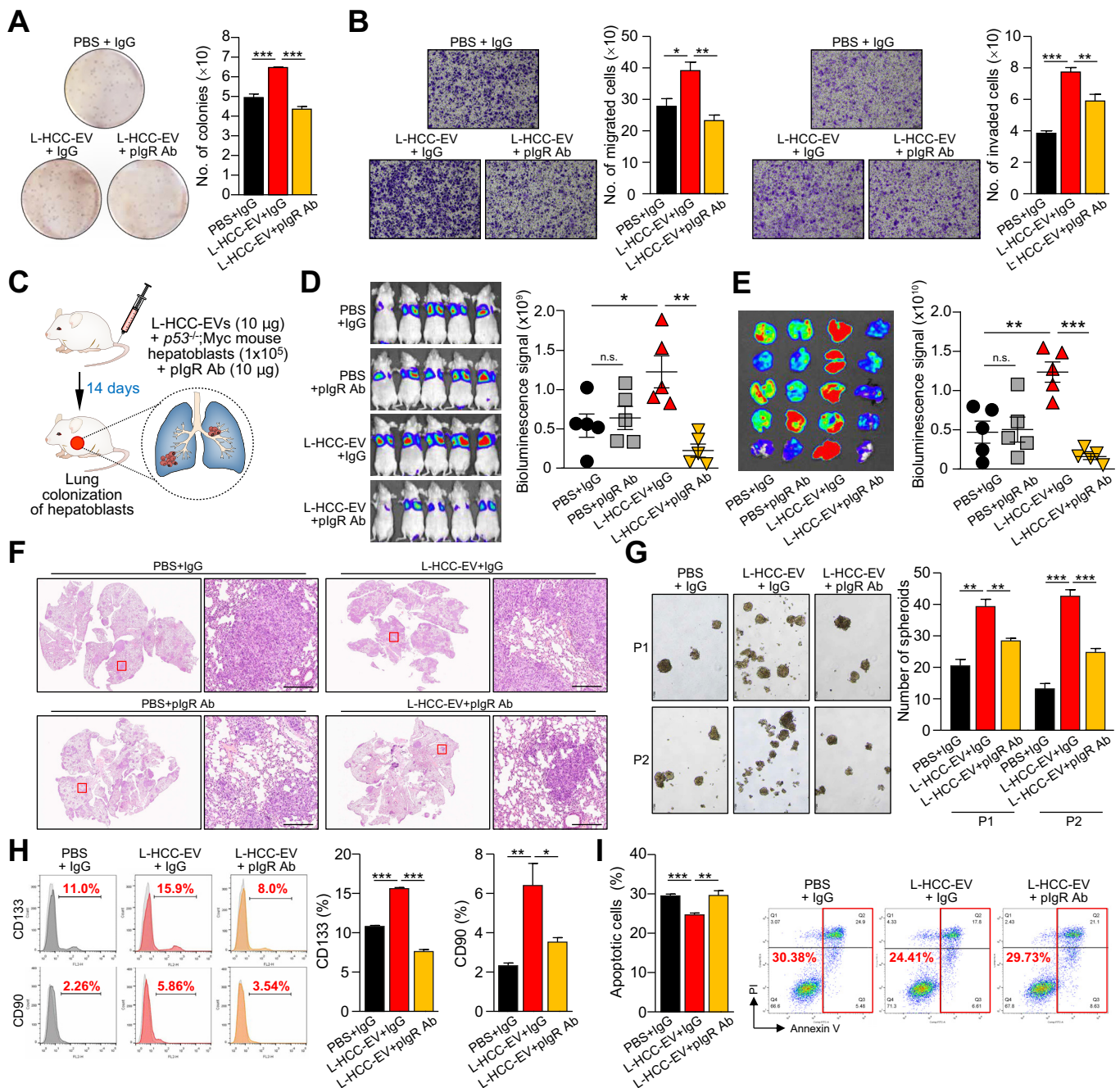


**Fig. 4. Anti-pIgR antibody hinders the ability of EVs from patients with HCC to enhance the cancer and cancer stemness properties of HCC cells.** PLC/PRF/5 cells treated with L-HCC-EVs in the presence of control IgG or anti-pIgR antibody were subjected to colony formation (A), migration and invasion (B) assays. (C) Schematic diagram of the experimental metastasis assay. (D) Bioluminescence imaging of animals at the end of experiment and quantification of the intensity of signals ( $n = 5$ ). (E) *Ex vivo* bioluminescence imaging of lungs. (F) Representative image of H&E staining of lung tissues. Scale bar, 200  $\mu\text{m}$ . Cells treated with L-HCC-EVs and with control IgG or anti-pIgR antibody were seeded for spheroid formation assays (G) and flow cytometry analysis to detect CD90 and CD133 expression (H). Histogram indicating the number of spheres formed per 1,000 cells. P1 and P2 represent passage 1 and 2, respectively. The percentage of positively stained CD90 and CD133 cells was plotted. (I) Cells pretreated as described and treated with sorafenib were stained with PI and annexin V-FITC. Flow cytometry analysis was conducted to determine the percentage of apoptotic cells. Data are presented as the mean  $\pm$  SEM. Student's *t* test for 2 groups was used. \* $p < 0.05$ ; \*\* $p < 0.01$ ; \*\*\* $p < 0.001$ . EVs, extracellular vesicles; HCC, hepatocellular carcinoma; L-HCC-EVs, EVs from patients with late HCC; PI, propidium iodide; pIgR, polymeric immunoglobulin receptor.

EVs exerted the highest potency in activating  $\beta$ -catenin expression, highlighting its potential in prompting malignant behaviors. The TOP/FOP reporter system demonstrated the activation of  $\beta$ -catenin activity by L-HCC-EVs (Fig. 6B). These observations

were further confirmed by immunofluorescence microscopy which revealed a notable increase in nuclear translocation of  $\beta$ -catenin in HCC cells following treatment with EVs with enhanced pIgR expression (Fig. 6C,D; Fig. S8A,B). Notably, the nuclear



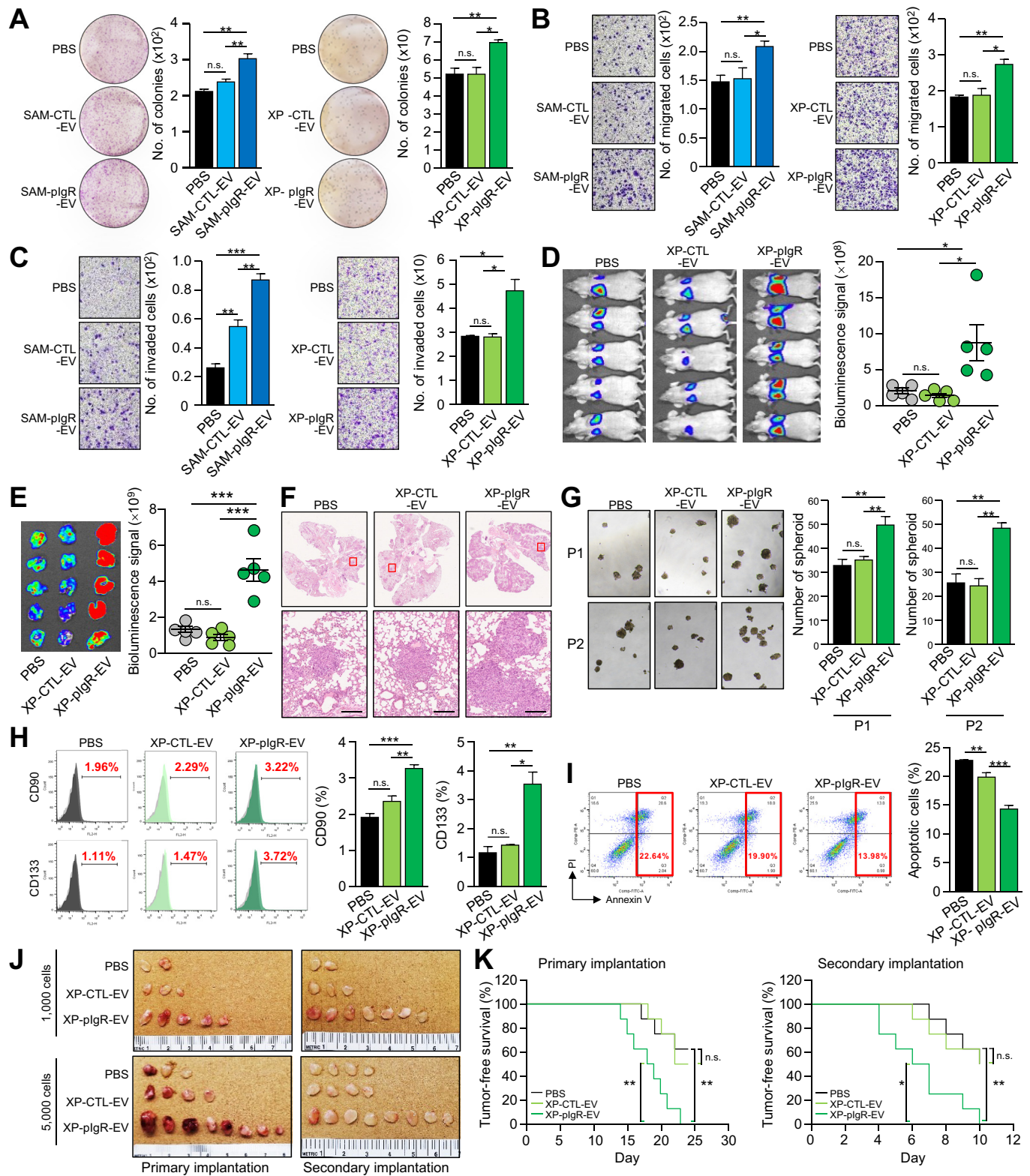


**Fig. 5. plgR-enriched EVs exert enhanced promoting effects on HCC cancer and cancer stemness properties.** Colony formation (A), migration (B) and invasion (C) assays were performed on PLC/PRF/5 cells treated with the indicated EVs from Huh7 cells and corresponding control EVs. (D) Luciferase-labeled murine p53<sup>-/-</sup>;Myc hepatoblasts were coinjected with the indicated EVs via the tail vein. Bioluminescence imaging of animals was performed 14 days post injection, and the luciferase signals were quantified. (E) Bioluminescence imaging of excised lungs. (F) Representative image of H&E staining of lung tissues. Scale bar, 200 μm. Cells treated with the indicated EVs were subjected to hepatosphere formation (G), flow cytometry analysis of the markers CD90 and CD133 (H) and apoptosis assays (I). Histogram indicating the number of spheres formed per 1,000 cells. P1 and P2 represent passage 1 and 2, respectively. The percentages of positively stained CD90<sup>+</sup> and CD133<sup>+</sup> cells and apoptotic cells were analyzed. (J) Image of tumors formed by PLC/PRF/5 cells pretreated with the indicated EVs in 2 rounds of implantation (n = 8). (K) Tumor-free survival curves of mice injected with 5,000 cells in the primary and secondary implantation are shown. Data are presented as the mean ± SEM. Student's *t* test was used for 2 groups, and a log-rank (Mantel-Cox) test was used for the survival curve. \**p* < 0.05; \*\**p* < 0.01; \*\*\**p* < 0.001; n.s., not significant. EVs, extracellular vesicles; HCC, hepatocellular carcinoma; plgR, polymeric immunoglobulin receptor.

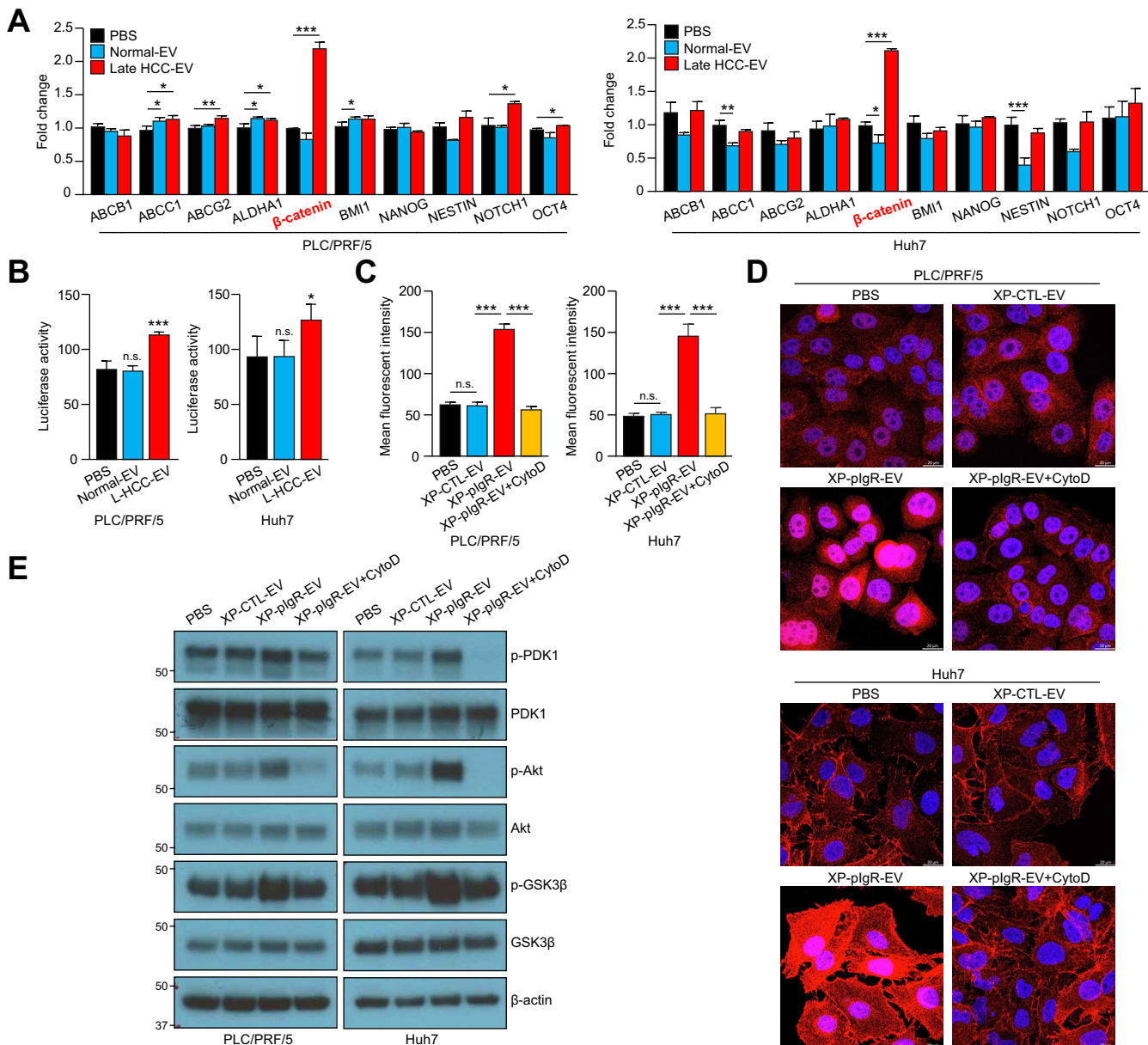


**Fig. 6. pIgR-enriched EVs activate  $\beta$ -catenin signaling through the PDK1/Akt/GSK3 $\beta$  axis in HCC cells.** (A) Expression of genes regulating cancer stemness and/or drug resistance in HCC cells treated with the indicated EVs was quantified by qPCR. Expression levels are expressed as the fold change compared to the PBS group. (B) The activity of  $\beta$ -catenin in HCC cells treated with the indicated EVs was analyzed using a TOP/FOP reporter assay. (C) HCC cells treated with EVs derived from stable XP-CTL and XP-pIgR cells in the absence or presence of CytoD were stained with anti- $\beta$ -catenin antibody and DAPI. Scale bar, 20  $\mu$ m. Histogram indicating the mean fluorescence intensity of the average nuclear  $\beta$ -catenin fluorescence captured by confocal microscopy (n = 10). (D) Representative fluorescence images. (E) Immunoblotting of PDK1, p-PDK1 (S241), Akt, p-Akt (S473), GSK3 $\beta$ , and p-GSK3 $\beta$  (S9) expression in PLC/PRF/5 cells treated with the indicated EVs;  $\beta$ -actin was used as the loading standard. Data are presented as the mean  $\pm$  SEM. Student's *t* test was used for 2 groups was used. \**p* <0.05; \*\**p* <0.01; \*\*\**p* <0.001; n.s., not significant. CytoD, cytochalasin D; EVs, extracellular vesicles; HCC, hepatocellular carcinoma; L-HCC-EVs, EVs from patients with late HCC; Normal-EV, EVs from healthy individuals; XP, expression vector.

translocation of  $\beta$ -catenin activated by L-HCC-EVs was suppressed by treatment with an endocytosis inhibitor, cytochalasin D, indicating that EVs were taken up by cells via endocytosis.

Phosphorylation of PDK1 leads to activation of Akt, which subsequently phosphorylates GSK3 $\beta$ , leading to stabilization and nuclear translocation of  $\beta$ -catenin.  $\beta$ -catenin signaling has been reported to regulate tumorigenesis, cancer stemness and chemoresistance.<sup>10</sup> XP-pIgR-EVs increased PDK1, Akt and GSK3 $\beta$  phosphorylation (Fig. 6E; Fig. S8C), and this activation was blocked by cytochalasin D, suggesting that cellular uptake of EVs

was required. In PLC/PRF/5 cells, the phosphorylation of Akt and GSK3 $\beta$  induced by XP-pIgR-EV was diminished by the Akt inhibitor IV and the  $\beta$ -catenin inhibitor PRI-724 (Fig. 7A). Functionally, treatment with these inhibitors abrogated the promoting effect of XP-pIgR-EVs on HCC cell growth and motility (Fig. 7B-D). Moreover, the effect of XP-pIgR-EVs on enhancing the *in vitro* self-renewal ability of PLC/PRF/5 cells, the percentage of CD90<sup>+</sup> and CD133<sup>+</sup> cells (Fig. 7E-F) and the sensitivity of cells to sorafenib (Fig. 7G) was diminished by cotreatment with the inhibitors. These findings demonstrate that pIgR-enriched EVs

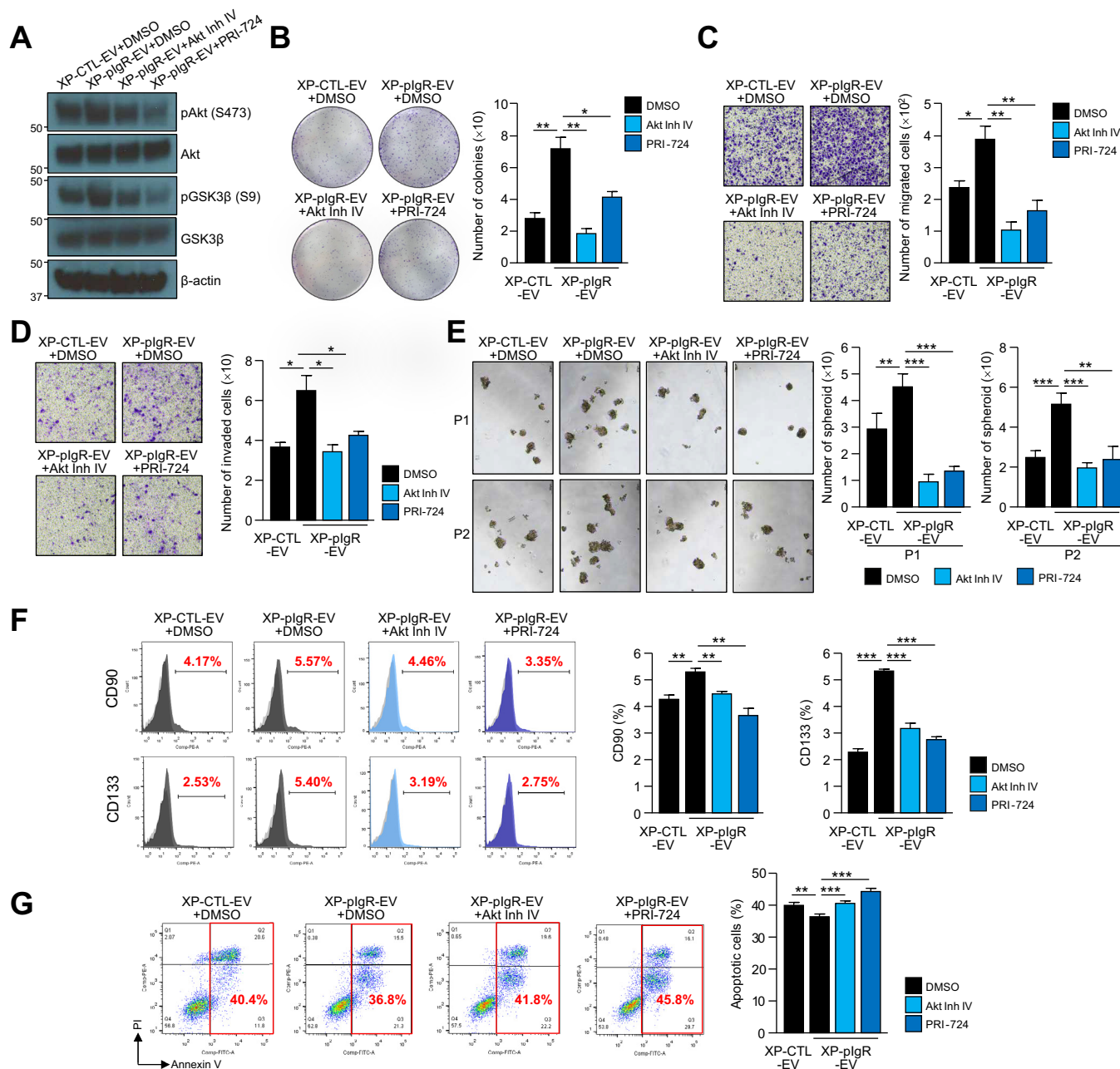


**Fig. 7. Inhibitors of Akt and  $\beta$ -catenin obstruct the promoting effect of plgR-enriched EVs on cancer and cancer stemness properties.** (A) Immunoblot showing Akt, phospho-Akt (S473), GSK3 $\beta$ , and p-GSK3 $\beta$  (S9) expression in PLC/PRF/5 cells treated with XP-CTL-EV and XP-plgR-EV and cotreated with either vehicle, Akt inhibitor IV (Akt Inh IV) or  $\beta$ -catenin inhibitor PRI-724. Anti- $\beta$ -actin was used as the loading standard. Treated cells were subjected to colony formation (B), migration (C) and invasion (D) assays. (E) Spheroid formation assays of the cells treated as described above were performed for 2 passages, P1 and P2, each with 1,000 cells. Flow cytometry analysis of CD90 $^+$  and CD133 $^+$  cells (F) and apoptotic cells (G) was performed. The percentages of CD90 $^+$  and CD133 $^+$  cells and apoptotic cells were plotted. Data are presented as the mean  $\pm$  SEM. Student's *t* test was used for 2 groups. \**p* < 0.05; \*\**p* < 0.01; \*\*\**p* < 0.001. EV, extracellular vesicle; XP, expression vector.

promote cancer and cancer stemness properties through the PDK1/Akt/GSK3 $\beta$ / $\beta$ -catenin axis.

**Targeting EV-plgR with a plgR neutralizing antibody is a potential therapeutic option for HCC**

The therapeutic effect of the anti-plgR antibody and sorafenib was tested in mice implanted with PDTXs that expressed plgR (Fig. 8A). Administration of anti-plgR antibody or sorafenib suppressed tumor growth compared to vehicle treatment

(Fig. 8B). Remarkably, cotreatment with sorafenib and anti-plgR antibody exerted the most potent inhibitory effect on tumor formation. We did not observe signs of distress or significant changes in the body weights of mice in any treatment group (Fig. 8C). The weight and dimensions of dissected tumors were significantly reduced in mice subjected to combined treatment with sorafenib and anti-plgR antibody (Fig. 8D). Immunohistochemistry analysis revealed no change in cellular plgR expression in tumors from different treatment groups, suggesting that

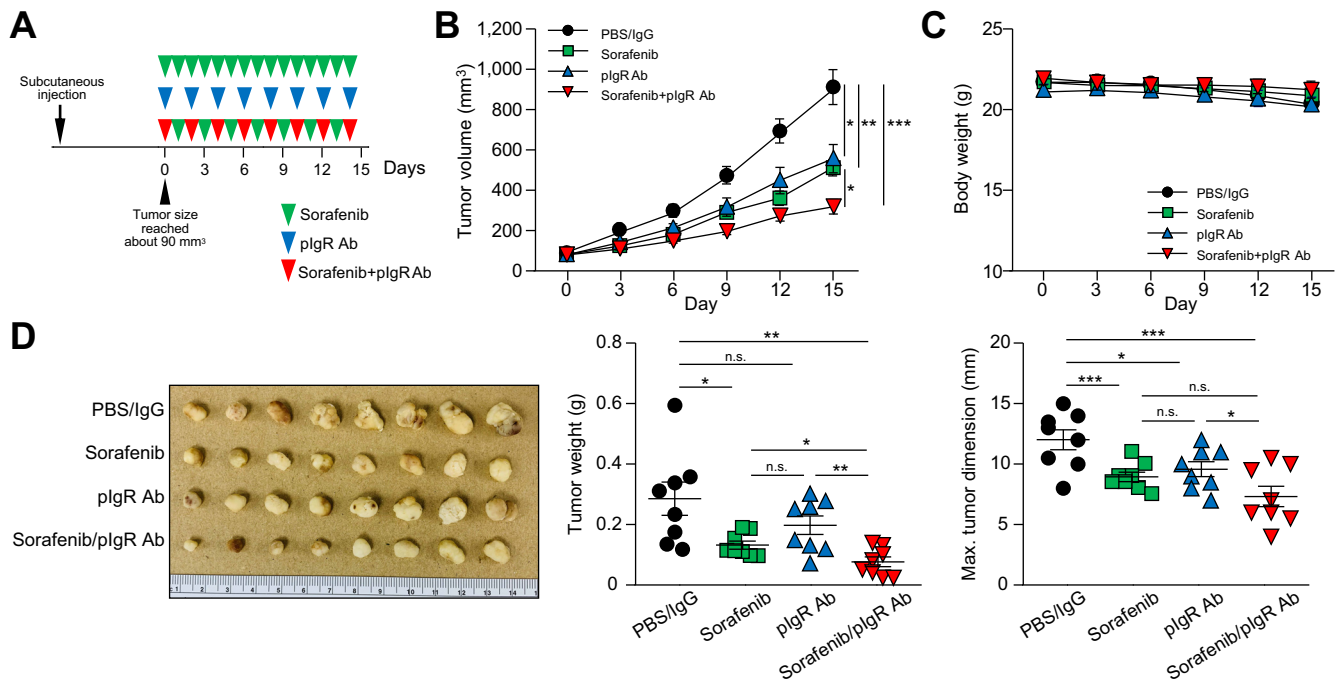


**Fig. 8. Treatment with sorafenib and plgR neutralizing antibody effectively inhibited the development of patient-derived tumor xenografts.** (A) Schematic diagram of the treatment regimen applied to mice subcutaneously implanted with patient-derived tumor xenografts. Mice were administered vehicle (DMSO in PBS and IgG), sorafenib, anti-plgR neutralizing antibody or a combination of sorafenib and anti-plgR neutralizing antibody. DMSO/PBS and sorafenib were administered daily via oral gavage. Control IgG and anti-plgR neutralizing antibody were injected peritoneally every 3 days ( $n = 8$ ). (B) Tumor growth was monitored and recorded every 3 days until the end of the experiment. Tumor volume was estimated and plotted against time. (C) The body weight of the mice was examined every 3 days until the experimental endpoint. The tumors were excised from the mice. (D) The weight and maximum dimension of tumors were measured and plotted. Data are presented as the mean  $\pm$  SEM. Two-way ANOVA with Turkey's test was used for multiple groups, or Student's  $t$  test was used for 2 groups. \* $p < 0.05$ ; \*\* $p < 0.01$ ; \*\*\* $p < 0.001$ ; n.s., not significant. Ab, antibody; plgR, polymeric immunoglobulin receptor.

the plgR neutralizing antibody acts by targeting EV-plgR but not endogenous plgR (data not shown).

### Discussion

Dysregulation of plgR was initially reported 45 years ago in malignantly transformed epithelial cells.<sup>11–13</sup> Since then, studies have reported contrasting expression of plgR in different human carcinomas,<sup>14–23</sup> and its role in prognostication of carcinomas remains inconclusive. plgR was previously implicated in metastasis by a study demonstrating its positive expression in hepatic metastatic tissues of colon carcinoma.<sup>24</sup> plgR has been reported to be mostly expressed in cholangiocytes, contributing to an increased secretory plgR level in the serum.<sup>25–27</sup> Immunohistochemistry of plgR revealed low to medium staining in hepatocytes but no staining in cholangiocytes based on data retrieved from the Human Protein Atlas. Comparison of tissue expression levels in cholangiocarcinoma (CCA) and HCC in the Cancer Genome Atlas and the Genotype-Tissue Expression databases revealed plgR expression in both carcinoma types, although there was no significant difference between tumorous and non-tumorous tissue. In line with the reported overexpression of plgR in HCC,<sup>8,9,28</sup> we observed increased transcript and protein levels of plgR in tumorous tissue compared with their counterparts, as well as in metastatic HCC cells compared with non-metastatic HCC cells and immortalized liver cells. Our findings suggest

that plgR is highly expressed in hepatocarcinoma cells and plays important oncogenic functions in HCC. More than 30 years ago, the detection of high levels of secretory components, which result from proteolytic cleavage of plgR, in the sera of patients with HCC was reported.<sup>27</sup> High levels of secretory plgR have also been detected in the sera of patients with bladder carcinoma, lung carcinoma and colonic carcinoma with liver metastasis.<sup>29–31</sup> Previously, the existence of plgR within EVs has been reported in both CCA and HCC.<sup>32</sup> In the present study, our data underscore the importance of EV-plgR in hepatocarcinogenesis and the potential of EV-plgR as a diagnostic and prognostic marker in HCC.

Although alterations in plgR expression have been detected in different cancer types, the understanding of the mechanism leading to dysregulation of plgR is limited. In HBV-related HCC, plgR interacts with and activates the Smad2/3 complex leading to epithelial-mesenchymal transition (EMT), providing a missing link between chronic inflammation and HCC metastasis.<sup>8</sup> Of note, it is possible that HBV-related chronic inflammation might contribute to changes in the microenvironment, which result in increased plgR expression and promote HCC metastasis. Additionally, a previous study suggested EV-plgR is a non-specific biomarker related to inflammation in CCA and HCC.<sup>32</sup> However, we did not observe an increased level of EV-plgR in either patients with HBV or cirrhosis. Thus, the involvement of EV-plgR in persistent inflammation and viral hepatitis requires further in-

depth investigation. The functional link between pIgR and EMT is also substantiated by its inverse correlation with E-cadherin expression in pancreatic cancer.<sup>33</sup> In addition, pIgR activates the Rac1/CDC42-MEK/ERK cascade to promote HCC tumor growth.<sup>9</sup> Another study revealed that bufalin inhibits HCC cell growth and motility by suppressing APOBEC3 and pIgR.<sup>34</sup> pIgR has been shown to exert oncogenic functions by activating ribosomal proteins in HCC.<sup>28</sup> However, these studies were either conducted in a physiologically irrelevant canine kidney cell line MDCK or in SMMC7721, BEL7404 and SKHEP1 cells which have been reported to be either HeLa cell contaminated or of endothelial origin.<sup>35</sup> Therefore, it is not surprising that neither endogenous pIgR nor EV-pIgR activated Smad2/3 signaling and induced EMT in HCC cells (data not shown).<sup>8</sup> Here, the EV-pIgR-induced PDK1/Akt/GSK3 $\beta$ / $\beta$ -catenin axis was observed in different HCC cell lines, regardless of their  $\beta$ -catenin mutation or activation status.<sup>36</sup> This mechanistic finding demonstrates how an immunoglobulin can be associated with tumorigenesis induced by EVs.

Intriguingly, during our establishment of stable clones with enhanced pIgR expression, we noticed the discrete molecular size of endogenous pIgR and EV-pIgR. Treatment of cells with the N-glycosylation inhibitor tunicamycin blocks the glycosylation of pIgR, revealing 2 distinct sizes of  $\sim$ 110 kDa and  $\sim$ 83 kDa.<sup>17,37</sup> Functionally, the glycosylation of pIgR aids in transcytosis and mediates the attachment of bacteria.<sup>37,38</sup> To date, the functional implications of non-glycosylated pIgR remain elusive. Our findings suggest that pIgR residing within EVs is in a non-glycosylated form. Importantly, our observation reveals an unreported oncogenic function of non-glycosylated EV-pIgR. However, the detailed regulatory mechanism of deglycosylation of pIgR during its packaging into EVs remains unanswered and requires further investigation.

Sorafenib is the first-line systemic therapy for patients with inoperable advanced HCC; unfortunately, the effect of sorafenib is modest, and most patients are highly resistant to sorafenib.<sup>39</sup> Other multikinase inhibitors, such as lenvatinib, regorafenib and carbozantinib, are not superior to sorafenib in terms of survival. In 2020, bevacizumab (anti-VEGF antibody) plus atezolizumab (anti-PD-L1 antibody) treatment was approved as a first-line treatment for unresectable HCC.<sup>40</sup> The combination strategy, which has a substantially better outcome than sorafenib alone, accentuates the advantages of combination treatment over monotherapy. Herein, our findings suggest that blockade of EV-pIgR with neutralizing antibodies either alone or in combination with sorafenib or other therapeutic agents may serve as a therapeutic option beyond the current limited treatments for HCC.

In conclusion, our study provides compelling evidence implicating patient-derived EVs with enhanced pIgR expression as key mediators of HCC cancer stemness and tumorigenesis. We also demonstrate that EV-pIgR exerts oncogenic functions via activation of  $\beta$ -catenin and that blockade of EV-pIgR with a neutralizing antibody is a potential treatment alternative.

### Abbreviations

Akt, protein kinase B; ANOVA, analysis of variance; CCA, cholangiocarcinoma; CSC, cancer stem cell; E-HCC-EVs, EVs from patients with early HCC; ELISA, enzyme-linked immunosorbent assay; EMT, epithelial-mesenchymal transition; EpCAM,

epithelial cell adhesion molecular; EVs, extracellular vesicles; GSK3 $\beta$ ; glycogen synthase kinase 3 $\beta$ ; HBV, hepatitis B virus; HCC, hepatocellular carcinoma; L-HCC-EVs, EVs from patients with late HCC; PBS, phosphate-buffered saline; PDK1, 3-phosphoinositide dependent kinase 1; PDTX, patient-derived tumor xenograft; pIgR, polymeric immunoglobulin receptor; qPCR, quantitative PCR; SAM, synergistic activation mediators; SEM, standard error of mean; XP, XPack expression vector.

### Financial support

The work was supported by in part by the funding of Research Grants Council Theme-Based Research Project on Liver Cancer Stemness (Project No. T12-704/16-R); The University of Hong Kong Seed Funding for Strategic Interdisciplinary Research Scheme (Project no.: 102009863 and 007000142).

### Conflict of interest

The authors have no conflict of interest to declare.

Please refer to the accompanying ICMJE disclosure forms for further details.

### Author's contributions

SKT, SWKW contributed equally to this work. Conceptualization: SKT, JWPY; Methodology: SKT, JWPY; Investigation: SKT, SWKW, JYTC, XM, THN, CLSY, ZL, HLF, AHNT, SKYM, TKWL; Resources: DKHW, LM, MY, CS, ION, PC, KZ, YG, JPY; Manuscript writing: SKT, JWPY; Funding Acquisition: JWPY.

### Data availability statement

We declare that all data involved in this study are available in the article along with the [supplementary materials](#).

### Acknowledgment

We acknowledge the assistance of The University of Hong Kong, Li Ka Shing Faculty of Medicine, Centre for PanOrOmic Sciences Imaging and Flow Cytometry Core for providing equipment needed for animal imaging and confocal microscopy. Raw data were acquired using Mass spectrometer maintained by CPOS Proteomics and Metabolomics Core. We also thank Centre for Comparative Medicine Research for providing animals and facility for animal experimentation and the Electron Microscope Unit for providing service and support needed for experiments involving electron microscope.

### Supplementary data

Supplementary data to this article can be found online at <https://doi.org/10.1016/j.jhep.2021.12.005>.

### References

*Author names in bold designate shared co-first authorship*

- [1] Villanueva A. Hepatocellular carcinoma. *N Engl J Med* 2019;380:1450–1462.
- [2] Alzahrani FA, El-Magd MA, Abdelfattah-Hassan A, Saleh AA, Saadeldin IM, El-Shetry ES, et al. Potential effect of exosomes derived from cancer stem cells and MSCs on progression of DEN-induced HCC in rats. *Stem Cells Int* 2018;2018:8058979.
- [3] Conigliaro A, Costa V, Lo Dico A, Saieva L, Buccheri S, Dieli F, et al. CD90+ liver cancer cells modulate endothelial cell phenotype through the release of exosomes containing H19 lncRNA. *Mol Cancer* 2015;14:155.

- [4] Kaetzel CS. The polymeric immunoglobulin receptor: bridging innate and adaptive immune responses at mucosal surfaces. *Immunol Rev* 2005;206:83–99.
- [5] **Mao X, Tey SK**, Yeung CLS, Kwong EML, Fung YME, Chung CYS, et al. Nidogen 1-enriched extracellular vesicles facilitate extrahepatic metastasis of liver cancer by activating pulmonary fibroblasts to secrete tumor necrosis factor receptor 1. *Adv Sci (Weinh)* 2020;7:2002157.
- [6] **Mao X, Zhou L**, Tey SK, Ma APY, Yeung CLS, Ng TH, et al. Tumour extracellular vesicle-derived Complement Factor H promotes tumorigenesis and metastasis by inhibiting complement-dependent cytotoxicity of tumour cells. *J Extracell Vesicles* 2020;10:e12031.
- [7] **Thery C, Witwer KW**, Aikawa E, Alcaraz MJ, Anderson JD, Andriantsitohaina R, et al. Minimal information for studies of extracellular vesicles 2018 (MISEV2018): a position statement of the International Society for Extracellular Vesicles and update of the MISEV2014 guidelines. *J Extracell Vesicles* 2018;7:1535750.
- [8] Ai J, Tang Q, Wu Y, Xu Y, Feng T, Zhou R, et al. The role of polymeric immunoglobulin receptor in inflammation-induced tumor metastasis of human hepatocellular carcinoma. *J Natl Cancer Inst* 2011;103:1696–1712.
- [9] **Yue X, Ai J, Xu Y, Chen Y**, Huang M, Yang X, et al. Polymeric immunoglobulin receptor promotes tumor growth in hepatocellular carcinoma. *Hepatology* 2017;65:1948–1962.
- [10] MacDonald BT, Tamai K, He X. Wnt/beta-catenin signaling: components, mechanisms, and diseases. *Dev Cell* 2009;17:9–26.
- [11] Harris JP, Caleb MH, South MA. Secretory component in human mammary carcinoma. *Cancer Res* 1975;35:1861–1864.
- [12] Poger ME, Hirsch BR, Lamm ME. Synthesis of secretory component by colonic neoplasms. *Am J Pathol* 1976;82:327–338.
- [13] Harris JP, South MA. Secretory component: a glandular epithelial cell marker. *Am J Pathol* 1981;105:47–53.
- [14] Zhou M, Liu C, Cao G, Gao H, Zhang Z. Expression of polymeric immunoglobulin receptor and its biological function in endometrial adenocarcinoma. *J Cancer Res Ther* 2019;15:420–425.
- [15] Wang X, Du J, Gu P, Jin R, Lin X. Polymeric immunoglobulin receptor expression is correlated with poor prognosis in patients with osteosarcoma. *Mol Med Rep* 2014;9:2105–2110.
- [16] Niu H, Wang K, Wang Y. Polymeric immunoglobulin receptor expression is predictive of poor prognosis in glioma patients. *Int J Clin Exp Med* 2014;7:2185–2190.
- [17] Arumugam P, Bhattacharya S, Chin-Aleong J, Capasso M, Kocher HM. Expression of polymeric immunoglobulin receptor and stromal activity in pancreatic ductal adenocarcinoma. *Pancreatol* 2017;17:295–302.
- [18] Ohkuma R, Yada E, Ishikawa S, Komura D, Kubota Y, Hamada K, et al. High expression levels of polymeric immunoglobulin receptor are correlated with chemoresistance and poor prognosis in pancreatic cancer. *Oncol Rep* 2020;44:252–262.
- [19] **Berntsson J, Lundgren S**, Nodin B, Uhlen M, Gaber A, Jirstrom K. Expression and prognostic significance of the polymeric immunoglobulin receptor in epithelial ovarian cancer. *J Ovarian Res* 2014;7:26.
- [20] Qi X, Li X, Sun X. Reduced expression of polymeric immunoglobulin receptor (pIgR) in nasopharyngeal carcinoma and its correlation with prognosis. *Tumour Biol* 2016;37:11099–11104.
- [21] Fristedt R, Gaber A, Hedner C, Nodin B, Uhlen M, Eberhard J, et al. Expression and prognostic significance of the polymeric immunoglobulin receptor in esophageal and gastric adenocarcinoma. *J Transl Med* 2014;12:83.
- [22] Khattar NH, Lele SM, Kaetzel CS. Down-regulation of the polymeric immunoglobulin receptor in non-small cell lung carcinoma: correlation with dysregulated expression of the transcription factors USF and AP2. *J Biomed Sci* 2005;12:65–77.
- [23] Krajci P, Meling GI, Andersen SN, Hofstad B, Vatn MH, Rognum TO, et al. Secretory component mRNA and protein expression in colorectal adenomas and carcinomas. *Br J Cancer* 1996;73:1503–1510.
- [24] **Liu F, Ye P**, Bi T, Teng L, Xiang C, Wang H, et al. COLORECTAL polymeric immunoglobulin receptor expression is correlated with hepatic metastasis and poor prognosis in colon carcinoma patients with hepatic metastasis. *Hepatogastroenterology* 2014;61:652–659.
- [25] Delacroix DL, Courtoy PJ, Rahier J, Reynaert M, Vaerman JP, Dive C. Localization and serum concentration of secretory component during massive necrosis of human liver. *Gastroenterology* 1984;86:521–531.
- [26] Tomana M, Kulhavy R, Mestecky J. Receptor-mediated binding and uptake of immunoglobulin A by human liver. *Gastroenterology* 1988;94:762–770.
- [27] Rossel M, Seilles E, Voigt JJ, Vuitton D, Legait N, Revillard JP. Polymeric Ig receptor expression in hepatocellular carcinoma. *Eur J Cancer* 1992;28A:1120–1124.
- [28] **Zhang Y, Zhang J**, Chen X, Yang Z. Polymeric immunoglobulin receptor (PIGR) exerts oncogenic functions via activating ribosome pathway in hepatocellular carcinoma. *Int J Med Sci* 2021;18:364–371.
- [29] Rossel M, Billerey C, Bittard H, Ksiazek P, Alber D, Revillard JP, et al. Alterations in polymeric immunoglobulin receptor expression and secretory component levels in bladder carcinoma. *Urol Res* 1991;19:361–366.
- [30] Kvale D, Norstein J, Meling GI, Borner OP, Brandtzaeg P, Langmark F, et al. Circulating secretory component in relation to early diagnosis and treatment of liver metastasis from colorectal carcinomas. *J Clin Pathol* 1992;45:568–571.
- [31] Rossel M, Brambilla E, Billaud M, Vuitton DA, Blanc-Jouvan F, Bichle S, et al. Nonspecific increased serum levels of secretory component in lung tumors: relationship to the gene expression of the transmembrane receptor form. *Am J Respir Cell Mol Biol* 1993;9:341–346.
- [32] Arbelaz A, Azkargorta M, Krawczyk M, Santos-Laso A, Lapitz A, Perugorria MJ, et al. Serum extracellular vesicles contain protein biomarkers for primary sclerosing cholangitis and cholangiocarcinoma. *Hepatology* 2017;66:1125–1143.
- [33] Kadaba R, Birke H, Wang J, Hooper S, Andl CD, Di Maggio F, et al. Imbalance of desmoplastic stromal cell numbers drives aggressive cancer processes. *J Pathol* 2013;230:107–117.
- [34] **Yang Z, Tao Y**, Xu X, Cai F, Yu Y, Ma L. Bufalin inhibits cell proliferation and migration of hepatocellular carcinoma cells via APOBEC3F induced intestinal immune network for IgA production signaling pathway. *Biochem Biophys Res Commun* 2018;503:2124–2131.
- [35] Rebouissou S, Zucman-Rossi J, Moreau R, Qiu Z, Hui L. Note of caution: contaminations of hepatocellular cell lines. *J Hepatol* 2017;67:896–897.
- [36] Ding Z, Shi C, Jiang L, Tolstykh T, Cao H, Bangari DS, et al. Oncogenic dependency on beta-catenin in liver cancer cell lines correlates with pathway activation. *Oncotarget* 2017;8:114526–114539.
- [37] Matsumoto N, Asano M, Ogura Y, Takenouchi-Ohkubo N, Chihaya H, Chung-Hsing W, et al. Release of non-glycosylated polymeric immunoglobulin receptor protein. *Scand J Immunol* 2003;58:471–476.
- [38] Mathias A, Cortes B. Recognition of gram-positive intestinal bacteria by hybridoma- and colostrum-derived secretory immunoglobulin A is mediated by carbohydrates. *J Biol Chem* 2011;286:17239–17247.
- [39] Niu L, Liu L, Yang S, Ren J, Lai PBS, Chen GG. New insights into sorafenib resistance in hepatocellular carcinoma: responsible mechanisms and promising strategies. *Biochim Biophys Acta Rev Cancer* 2017;1868:564–570.
- [40] Finn RS, Qin S, Ikeda M, Galle PR, Ducreux M, Kim T-Y, et al. Atezolizumab plus bevacizumab in unresectable hepatocellular carcinoma. *N Engl J Med* 2020;382(20):1894–1905.